Spontaneous adaptation of ion selectivity in a bacterial flagellar motor

Pietro Ridone[1], Yoshiyuki Sowa[2,3], Matthew A. B. Baker[1,4*]

[1]School of Biotechnology and Biomolecular Sciences, University of New South Wales, Sydney, Australia.

[2]Department of Frontier Bioscience, Hosei University, Tokyo, Japan.

[3]Research Center for Micro-Nano Technology, Hosei University, Tokyo, Japan.

[4]CSIRO Synthetic Biology Future Science Platform, Brisbane, Australia.

*correspondence: matthew.baker@unsw.edu.au

ABSTRACT

Motility provides a selective advantage to many bacterial species and is often achieved by rotation of flagella that propel the cell towards more favourable conditions. In most species, the rotation of the flagellum, driven by the Bacterial Flagellar Motor (BFM), is powered by H^+ or Na^+ ion transit through the torque-generating stator subunit of the motor complex. The ionic requirements for motility appear to have adapted to environmental changes throughout history but the molecular basis of this adaptation, and the constraints which govern the evolution of the stator proteins are unknown. Here we use CRISPR-mediated genome engineering to replace the native H^+-powered stator genes of *E. coli* with a compatible sodium-powered stator set from *V. alginolyticus* and subsequently direct the evolution of the stators to revert to H^+-powered motility. Evidence from whole genome sequencing indicates both flagellar- and non-flagellar-associated genes that are involved in longer-term adaptation to new power sources. Overall, transplanted Na^+- powered stator genes can spontaneously incorporate novel mutations that allow H^+-motility when environmental Na^+ is lacking.

INTRODUCTION

Bacterial motility via the flagellar motor represents one of the earliest forms of locomotion. This rotary motility imparts such significant selective advantage (Roszak and Colwell 1987, Fraebel, Mickalide et al. 2017) that resources are allocated to chemotaxis even in the absence of nutrient gradients (Gude, Pince et al. 2020, Ni, Colin et al. 2020). Furthermore, the evolutionary origins, and subsequent adaptation of the motor are of significant scientific and public interest (Pallen and Matzke 2006), since the BFM holds prominence as an ancient, large, molecular complex of high sophistication.

The torque that drives the BFM is supplied by motor-associated transmembrane protein-complexes known as stators. The stator complex, an asymmetric heteroheptamer (in *E. coli:* $MotA_5MotA_2$) most likely acts itself as a miniature rotating nanomachine coupling ion transit to rotation (Deme, Johnson et al. 2020, Santiveri, Roa-Eguiara et al. 2020). The stators are essential for motility, as they drive rotation, and are accessible for studies in experimental evolution due to their unambiguous role in connecting a specific environmental cue (presence of the coupling ion) to an easily discernible phenotype (cell swimming). Furthermore, the stators have been subject to protein engineering approaches for many years, in particular the synthesis of chimeric stator constructs that enable the motor of *E. coli*, natively proton-driven, to be powered by sodium ion flow (Asai, Yakushi et al. 2003).The majority of stators are proton driven, but many that are sodium-driven can be found in nature, and this divergence is presumed to have occurred in the distant past (Takekawa, Isumi et al. 2019, Islam, Lin et al. 2020, Lai, Ridone et al. 2020). Past reports have argued that H^+-coupled motility diverged from Na^+-coupled machinery in ancestral times (Takekawa, Nishiyama et al. 2015), but the molecular basis for this adaptation, and the evolutionary landscape that constrains stator adaptation remains unclear.

In order to simulate the effects of natural evolution on stator adaptation we designed an experiment where an *E. coli* strain, expressing only a sodium-powered stator, would be introduced to a non-lethal environment (soft agar swim plate) which lacked the power source for the stator (Na^+). Our hypothesis was that the population would undergo selection for upmotile variants, adapting its stators to function in the new environment.

We used genomic editing techniques (no-SCAR CRISPR/Cas9 (Reisch and Prather 2015) and λ-Red (Datsenko and Wanner 2000)) to replace the native *motA motB* stator genes of the *E. coli* BFM with chimeric sodium-powered *pomA potB* (henceforth *pots*) stator genes derived from *V. alginolyticus* (Asai, Yakushi et al. 2003). We transplanted the *pots* stator genes at the same location and orientation of the native *motA motB* locus to preserve the native genomic context of the motile RP437 *E. coli* strain. We then examined which genetic changes occurred during growth on soft-agar in depleted sodium, that is, under selective pressure for proton-driven motility. We performed our directed evolution experiments of our *pots E.coli* strain in the absence of antibiotics to avoid additional, undesired selective pressures (Baym, Lieberman et al. 2016).

RESULTS

Preparation and Directed Evolution of a Na^+ powered E.coli strain

The RP437 strain was edited to carry the chimeric *pomApotB* stator genes in place of the native *E. coli motAmotB* genes (henceforth *motAB*; Fig. 1A) via the no-SCAR Method (Reisch and Prather 2015) and traditional λ-Red recombineering respectively (Supplementary Figs. 1-3). Following verification of successful editing by colony PCR and Sanger Sequencing (Supplementary Fig. 2AB), a no-SCAR Pots clone was selected and tested on swim plates (Fig. 1B). The edited strain was able to swim on sodium-rich (85 mM NaCl) soft agar plates but not on potassium-rich sodium-poor (67 mM KCl, ~8 mM [Na^+]) plates (Fig. 1B). This edited strain exhibited the same swimming behaviour as the control stator-less strain with motility restored via an inducible plasmid vector that could express the *Pots* construct (RP6894 Δ*motAB* + pSHU1234).

We next challenged this *pots* strains to survive on K^+ based soft agar for prolonged periods (Fig. 1C). Motile subpopulations arose spontaneously from inoculated colonies within a few days. Cells from the edge of these motile flares were passaged onto fresh swim agar for up to 5 passages at 3-4 days intervals (Supplementary Fig. 4). When multiple flares occurred in a single swim ring, each was individually passaged (Fig. 1C), and could be recapitulated (Fig. 1D). Directed evolution consistently generated swimming flares when *pots* clones were cultured on agar containing yeast extract and tryptone (~8 mM [Na^+]), but not on minimal media (~ 1mM total [Na^+]) or when the *pots* construct was expressed from a plasmid

92 (Supplementary Fig. 5). One *pots* strain generated using λ-Red methods (Datsenko
93 and Wanner 2000), which carried the native *V. alginolyticus pomA* promoter, also
94 successfully produced flares (Supplementary Fig. 6).

95 Lineages were selected for WGS after a preliminary screening for mutations in the
96 stator genes by Sanger-sequencing PCR amplicons spanning the genomic
97 *pomApotB* locus (Fig. 2A). Variant calling to the MG1655 reference genome was
98 used to compare single nucleotide polymorphisms (SNPs) between members of the
99 same lineage. Our intended *pomApotB* edit was the only difference between the
100 RP437 and *Pots* genomes, indicating that neither no-SCAR nor λ-Red editing had
101 resulted in off-target edits (Fig. 2A). 153 SNPs were called as variants between our
102 experimental parent RP437 and the MG1655 reference which were shared across all
103 lineage members (Supplementary Table).

104 Lineages whose descendants could swim in reduced sodium had mutations at the
105 *pots* locus (L3.3-4-5: PotB G20V; L6.4-5: PomA L183F; L8.3-4-5: PotB G20W). In
106 contrast, lineages passaged only on 85 mM Na^+ agar (L1 & L2) accumulated
107 mutations not in stators but in the flagellar components. Lineages passaged on ~8
108 mM sodium-poor agar whose descendants could not swim (L4) had no mutations on
109 any flagellar genes.

110 To examine mutation reproducibility in the stators at higher throughput, we subjected
111 55 *pots* colonies to directed evolution in 8 mM [Na^+] agar. These yielded a total of 42
112 flares within the first 3 days of incubation, which were then passaged four more
113 times at 3-day intervals. At the end of this experiment we selected the 20 terminal
114 lineage members which produced the largest swim rings and Sanger-sequenced
115 them at the *pots* locus. For these we observed a total of 5 mutations in *pomA* (S25C,
116 D31N, P177A, P177Q and L183F) and one more new mutation in *potB* (L36Q).

117 Over the course of these experiments, we found that three stator residues underwent
118 mutation at the same site twice (PomA L183F (2x), PomA P177A & P177Q, PotB
119 G20V & G20W). WGS revealed that the *pitA* gene had mutated in three separate
120 lineages (L2.5, L3.5, L8.5) with one of the mutations occurring twice (PitA
121 W112*Stop).

122 To test for the capacity for reversion, we took sequenced lineages that swam in 8
123 mM [Na^+] agar (L3.3-4-5, L6.4-5, L8.3-4-5) and reintroduced them to an environment
124 with 85 mM [Na^+] (Supplementary Fig. 7A). After 10 rounds of daily passaging, no

125 reversion in the mutants that had enabled low-sodium swimming was observed, with
126 only a single additional mutation gained: a *potB* T21A mutation in the terminal
127 descendant of *potB* G20W *pitA* W112*stop (L8.5).

128 We further tested whether evolution could be more easily directed on minimal media
129 when starting from a more favourable vantage. We examined all stator mutants that
130 swam on 8 mM [Na^+] plates in conditions of further sodium scarcity (minimal media: 1
131 mM [Na^+]). Initially, only the strains with *potB* G20V and *pomA* P177Q mutations
132 could swim, and this capacity was maintained following five passages over 12 days.
133 Sanger sequencing revealed that the terminal descendant of p*otB* G20V *pitA* G432R
134 mutant (L3.5) gained a further mutation in *pomA* (M20L) (Supplementary Fig.7B). A
135 summary of all stator gene mutations obtained from all directed evolution
136 experiments is provided in Fig. 2D.

137 Finally, we characterized rotational phenotypes of the parent and evolved strains in
138 the presence and absence of sodium using a tethered cell assay (Fig. 2B,
139 Supplementary Fig. 8). The rotation speeds of single cells were measured under
140 sodium-free 67mM KCl or 85mM NaCl buffer conditions and also tested in presence
141 of 100 μM of the sodium-blocker phenamil (Atsumi, Sugiyama et al. 1990). The *potB*
142 G20V (L3.3) actively rotated in sodium-free buffers and in presence of 100 μM
143 Phenamil (Fig.2B) – indicating sodium-free rotation and a disrupted phenamil binding
144 site (Fig.2B). We confirmed the PotB G20V H^+-powered phenotype by introducing
145 the same point mutation (GGG to GTG) on our plasmid vector (pPots) and testing
146 motility in tethered cell assay when the protein was expressed in the stator-less
147 Δ*motAB* RP6894 (Fig.2C).

148 We mapped mutants to their homologous position on the recently published high-
149 resolution *B. subtilis* $MotA_5B_2$ structure (Deme, Johnson et al. 2020) (Fig. 2EF). All
150 stator mutations accumulated at sites proximal to or within the predicted ion-
151 transport pore, at the interface between the PotB transmembrane domain and the
152 third and fourth transmembrane domains of PomA (Fig. 2F).

153 **DISCUSSION**

154 In our experiments we observed repeated mutation around the pore of the stator
155 complex in response to ion-scarcity in the environment. We confirmed phenotypic
156 changes by measuring rotation in the absence of sodium and in the presence of the
157 sodium channel blocker phenamil. Our strains adapted quickly to drive rotation in a

158 sodium-poor environment within 2 weeks indicating that the stators are highly
159 adaptive.

160 Ni et al. observed that evolutionary adaptation of motility occurs via remodeling of
161 the checkpoint regulating flagellar gene expression (Ni, Ghosh et al. 2017). Their
162 experiments tracked adaptive changes in swim plates, matching our experiments,
163 however their only selection criteria were for improved swimming in an unhindered
164 swimming population. In agreement with our results (*fliM* A161V), they found *fliM*
165 *(*M67I and T192N*)* to be the amongst the first genes to mutate in the improved
166 swimmer population but they did not report any changes in *flgL* (ΔA57-Q58), nor,
167 significantly, did they see any mutations in any stator genes.

168 In contrast, our *E. coli pots* strain faced selective pressure from ion scarcity. Our
169 scenario is reminiscent of previous semi-solid agar experimental evolution studies on
170 the adaptation of antibiotic resistance and recapitulates similar results. In the MEGA
171 plate experiments of Baym et al., they similarly saw that the phosphate transporter
172 *pitA* was repeatedly mutated, often to a frameshifted or nonsense variant (Baym,
173 Lieberman et al. 2016). In similar experiment the isocitrate dehydrogenase *icd* was
174 also seen to mutate often (Fraebel, Mickalide et al. 2017).

175 Mutations in stators are known to affect ion usage and may confer dual-ion coupling
176 capacity. For example, the substate preference of the *B. alcalophilus* MotPS stator
177 (Na^+/K^+ and Rb^+) was changed with the single mutation M33L in MotS, causing the
178 loss of both K^+- and Rb^+-coupling motility in E. coli (Terahara, Sano et al. 2012).
179 Similarly a bi-functional *B. clausii* MotAB stator (Na^+/H^+) triple mutant (MotB V37L,
180 A40S and G42S) was selective only for sodium ions while the combination of
181 mutations G42S, Q43S and Q46A made MotB selective only for H^+ (Terahara,
182 Krulwich et al. 2008).

183 Except the previously reported variant *pomA* L183F (Sudo, Terashima et al. 2009),
184 none of the other mutations we report have been observed in previous studies
185 involving random mutagenesis in *motB* using ethylmethane sulfonate (Garza, Harris-
186 Haller et al. 1995), or by mutagenesis in the *pomA* gene by using hydroxylamine
187 (Kojima, Kuroda et al. 1999), or in *potB* using error-prone PCR (Ishida, Ito et al.
188 2019). Adaptation of plasmid-encoded chimeric stator genes (Nishino, Onoue et al.
189 2015) and wild-type stator genes (Takekawa, Nishiyama et al. 2015) has been
190 previously reported. One advantage of editing sodium stators onto the *E. coli*

genome is that we can direct the evolution of sodium-stators *in vivo* – something not possible in *Vibrio sp.* since the cells do not survive at low sodium. Conversely, it is difficult to direct evolution towards reversion because it is not possible, particularly in *E. coli*, to drastically reduce the proton concentration to incentivise the stators' use of sodium. Nevertheless, the fact that no revertants were observed agrees with previous work suggesting that requirements for Na^+ binding are more strict than for H^+ binding, and that mutations that convert a Na+ motor to an H+ are more accessible than the reverse (Hase, Fedorova et al. 2001, Mulkidjanian, Galperin et al. 2008).

We observed a convergence of mutations on the stator genes and even to the very same nucleotide (GAG (L) to GAA (F) in two separate *pom*A L183F lineages). That this was from a clonal population under identical environmental constraints suggests that adaptation of the stators is prioritized in changing environments. Mutation of pore-proximal residues into hydrophobic residues (eg. G20V) might hint at a mechanism for varying constrictions in the pore to alter the efficiency of ion binding.

Motility confers a fitness advantage that is worth significant energetic investment despite the high cost of synthesizing the flagellar machinery (Colin and Sourjik 2017, Ni, Colin et al. 2020). This advantage can only be seized if the correct ions are available for stator-conversion into torque. CRISPR/Cas9 has become a widespread method used for precise genomic edits, yet the reversion of such edits appears rapid and gene targeted. Here, ion scarcity supplied a strong selective pressure that allowed us to identify novel mutations correlated with altered ion-specificity. Our transplant of an unfit protein and the cells' rapid reversion of this edit demonstrates tight evolutionary regulation of the stator subunit in an ancient molecular complex.

MATERIALS AND METHODS

Starting strains and plasmids.

E. coli strain RP437 was used as the parent strain for genomic editing experiments (Block, Blair et al. 1989). The pSHU1234 (hereby pPots) plasmid encoding *pomA* and *potB* (Ishida, Ito et al. 2019) was used as the template to generate the double stranded donor DNA. This was used to replace the *motA* and *motB* gene on the RP437 chromosome. Liquid cell culturing was done using LB broth (NaCl or KCl, Yeast Extract, Bacto Tryptone). Cells were cultured on agar plates composed of LB Broth and 1% Bacto Agar (BD, U.S.A.). Swim plate cultures were performed on the

224 same substrates adjusted for agar content (0.3% Bacto Agar). A list of primers and
225 PCR protocols used in this work is provided in Supplementary Fig. 9.

226 **Editing E. coli with Cas9-assisted Recombineering.**

227 This procedure was adapted from the *No-SCAR* method (Reisch and Prather 2015) .
228 The target strain to be edited (*E.coli* RP437) was sequentially transformed first with
229 the pKD-sgRNA-3'MotA (Sm^+) plasmid, encoding a sgRNA sequence directed at the
230 3' end of *motA*, and then with the pCas9cr4 (Cm^+) plasmid to yield a parent strain
231 harboring both plasmids. The overlap extension PCR technique (Higuchi, Krummel
232 et al. 1988) was employed to assemble linear double stranded DNA molecules
233 (dsDNA) using 3 starting dsDNA fragments. The resulting donor DNA was
234 electroporated in the plasmid-bearing host and the successfully edited clones were
235 selected via colony PCR and Sanger sequencing of the *motAB* locus.

236 **Construction of Pots by λ-Red Recombineering**

237 Chromosomal replacement from *motAB* to *pomApotB* was achieved by using a λ
238 Red recombination system, with plasmid pKD46 encoding the Red system and
239 positive selection for the recovery of swimming ability (Kinosita, Ishida et al. 2020).
240 Motile clones were selected by isolating motile flares on swim plates (Supplementary
241 Fig.4).

242 **Tethered cell assay preparation and analysis**

243 The tethered cell assay was performed as previously described (Nishiyama and
244 Kojima 2012). The tethered cells time lapse videos were recorded at 40x
245 magnification on a phase contrast microscope (Nikon). Time lapse videos were
246 collected using a camera (Chameleon3 CM3, Point Grey Research) recording 20s-
247 long videos at 20 frames per second. A custom LabView software (Ishida, Ito et al.
248 2019, Islam, Lin et al. 2020) was employed as previously reported to estimate
249 specific rotational parameters of the tethered cells such as rotation frequency
250 (speed), clockwise and counterclockwise bias and switching frequency. Statistical
251 analysis and visualization of the data was performed using Graph Pad Prism 8.

252 **Single Nucleotide Polymorphism (SNP) analysis**

253 Whole genome sequencing of 22 *E. coli* strains was performed using a MiSeq 2 x
254 150bp chip on an Illumina sequencing platform. Sequencing was carried out at the
255 Ramaciotti Centre for Genomics, Kensington and delivered as demultiplexed fastQ
256 files (Quality Control: >80% bases higher than Q30 at 2×150 bp). The SNP calling
257 and analysis was performed using Snippy (Seemann 2015, Bush, Foster et al.

258 2020). The short reads from sequencing were aligned to the MG1655 reference *E.*
259 *coli* genome (GenBank: U00096.2) and to a synthetic genome based on MG1655,
260 edited to contain the Pots stator sequences from pPots (*pomA*/*potB*) at the *motAB*
261 locus.

262 **AUTHOR CONTRIBUTIONS**

263 PR and MABB designed experiments and executed experiments in strain editing,
264 molecular biology and microbiology. YS executed experiments in strain editing.
265 MABB executed bioinformatics surrounding variant calling. MB supervised the
266 design, execution and writing of the project. All authors contributed to writing and
267 revision of the manuscript.

268 **ACKNOWLEDGEMENTS**

269 We would like to acknowledge Myu Yoshida and Rie Ito for technical assistance.

270 **FUNDING**

271 YS was supported by JSPS KAKENHI (JP18H02475 and JP20K06564), MEXT
272 KAKENHI (JP19H05404) and Takeda Science Foundation. MABB was supported by
273 a UNSW Scientia Research Fellowship, a CSIRO Synthetic Biology Future Science
274 Platform 2018 Project Grant, and ARC Discovery Project DP190100497.

275 **REFERENCES**

276 Asai, Y., T. Yakushi, I. Kawagishi and M. Homma (2003). "Ion-coupling determinants of Na+-driven
277 and H+-driven flagellar motors." J Mol Biol **327**(2): 453-463.
278 Atsumi, T., S. Sugiyama, E. J. Cragoe, Jr. and Y. Imae (1990). "Specific inhibition of the Na(+)-driven
279 flagellar motors of alkalophilic Bacillus strains by the amiloride analog phenamil." J Bacteriol **172**(3):
280 1634-1639.
281 Baym, M., T. D. Lieberman, E. D. Kelsic, R. Chait, R. Gross, I. Yelin and R. Kishony (2016).
282 "Spatiotemporal microbial evolution on antibiotic landscapes." Science **353**(6304): 1147-1151.
283 Block, S. M., D. F. Blair and H. C. Berg (1989). "Compliance of bacterial flagella measured with optical
284 tweezers." Nature **338**(6215): 514-518.
285 Bush, S. J., D. Foster, D. W. Eyre, E. L. Clark, N. De Maio, L. P. Shaw, N. Stoesser, T. E. A. Peto, D. W.
286 Crook and A. S. Walker (2020). "Genomic diversity affects the accuracy of bacterial single-nucleotide
287 polymorphism-calling pipelines." Gigascience **9**(2).
288 Colin, R. and V. Sourjik (2017). "Emergent properties of bacterial chemotaxis pathway." Curr Opin
289 Microbiol **39**: 24-33.
290 Datsenko, K. A. and B. L. Wanner (2000). "One-step inactivation of chromosomal genes in Escherichia
291 coli K-12 using PCR products." Proc Natl Acad Sci U S A **97**(12): 6640-6645.
292 Deme, J. C., S. Johnson, O. Vickery, A. Aron, H. Monkhouse, T. Griffiths, R. H. James, B. C. Berks, J. W.
293 Coulton, P. J. Stansfeld and S. M. Lea (2020). "Structures of the stator complex that drives rotation of
294 the bacterial flagellum." Nat Microbiol **5**(12): 1553-1564.
295 Deme, J. C., S. Johnson, O. Vickery, A. Muellbauer, H. Monkhouse, T. Griffiths, R. H. James, B. C.
296 Berks, J. W. Coulton, P. J. Stansfeld and S. M. Lea (2020). "Structures of the stator complex that
297 drives rotation of the bacterial flagellum." Nature Microbiology **5**(12): 1553-+.

298 Fraebel, D. T., H. Mickalide, D. Schnitkey, J. Merritt, T. E. Kuhlman and S. Kuehn (2017).
299 "Environment determines evolutionary trajectory in a constrained phenotypic space." Elife **6**.
300 Garza, A. G., L. W. Harris-Haller, R. A. Stoebner and M. D. Manson (1995). "Motility protein
301 interactions in the bacterial flagellar motor." Proc Natl Acad Sci U S A **92**(6): 1970-1974.
302 Gude, S., E. Pince, K. M. Taute, A. B. Seinen, T. S. Shimizu and S. J. Tans (2020). "Bacterial coexistence
303 driven by motility and spatial competition." Nature **578**(7796): 588-592.
304 Hase, C. C., N. D. Fedorova, M. Y. Galperin and P. A. Dibrov (2001). "Sodium ion cycle in bacterial
305 pathogens: evidence from cross-genome comparisons." Microbiol Mol Biol Rev **65**(3): 353-370, table
306 of contents.
307 Higuchi, R., B. Krummel and R. K. Saiki (1988). "A general method of in vitro preparation and specific
308 mutagenesis of DNA fragments: study of protein and DNA interactions." Nucleic Acids Res **16**(15):
309 7351-7367.
310 Ishida, T., R. Ito, J. Clark, N. J. Matzke, Y. Sowa and M. A. B. Baker (2019). "Sodium-powered stators
311 of the bacterial flagellar motor can generate torque in the presence of phenamil with mutations
312 near the peptidoglycan-binding region." Mol Microbiol **111**(6): 1689-1699.
313 Islam, M. I., A. Lin, Y. W. Lai, N. J. Matzke and M. A. B. Baker (2020). "Ancestral Sequence
314 Reconstructions of MotB Are Proton-Motile and Require MotA for Motility." Front Microbiol **11**:
315 625837.
316 Kinosita, Y., T. Ishida, M. Yoshida, R. Ito, Y. V. Morimoto, K. Goto, R. M. Berry, T. Nishizaka and Y.
317 Sowa (2020). "Distinct chemotactic behavior in the original Escherichia coli K-12 depending on
318 forward-and-backward swimming, not on run-tumble movements." Sci Rep **10**(1): 15887.
319 Kojima, S., M. Kuroda, I. Kawagishi and M. Homma (1999). "Random mutagenesis of the pomA gene
320 encoding a putative channel component of the Na(+)-driven polar flagellar motor of Vibrio
321 alginolyticus." Microbiology (Reading) **145 (Pt 7)**: 1759-1767.
322 Lai, Y. W., P. Ridone, G. Peralta, M. M. Tanaka and M. A. B. Baker (2020). "Evolution of the Stator
323 Elements of Rotary Prokaryote Motors." J Bacteriol **202**(3).
324 Mulkidjanian, A. Y., M. Y. Galperin, K. S. Makarova, Y. I. Wolf and E. V. Koonin (2008). "Evolutionary
325 primacy of sodium bioenergetics." Biol Direct **3**: 13.
326 Ni, B., R. Colin, H. Link, R. G. Endres and V. Sourjik (2020). "Growth-rate dependent resource
327 investment in bacterial motile behavior quantitatively follows potential benefit of chemotaxis." Proc
328 Natl Acad Sci U S A **117**(1): 595-601.
329 Ni, B., B. Ghosh, F. S. Paldy, R. Colin, T. Heimerl and V. Sourjik (2017). "Evolutionary Remodeling of
330 Bacterial Motility Checkpoint Control." Cell Rep **18**(4): 866-877.
331 Nishino, Y., Y. Onoue, S. Kojima and M. Homma (2015). "Functional chimeras of flagellar stator
332 proteins between E-coli MotB and Vibrio PomB at the periplasmic region in Vibrio or E-coli."
333 Microbiologyopen **4**(2): 323-331.
334 Nishiyama, M. and S. Kojima (2012). "Bacterial motility measured by a miniature chamber for high-
335 pressure microscopy." Int J Mol Sci **13**(7): 9225-9239.
336 Pallen, M. J. and N. J. Matzke (2006). "From The Origin of Species to the origin of bacterial flagella."
337 Nat Rev Microbiol **4**(10): 784-790.
338 Reisch, C. R. and K. L. Prather (2015). "The no-SCAR (Scarless Cas9 Assisted Recombineering) system
339 for genome editing in Escherichia coli." Sci Rep **5**: 15096.
340 Roszak, D. B. and R. R. Colwell (1987). "Survival strategies of bacteria in the natural environment."
341 Microbiol Rev **51**(3): 365-379.
342 Santiveri, M., A. Roa-Eguiara, C. Kühne, N. Wadhwa, H. C. Berg, M. Erhardt and N. M. I. Taylor (2020).
343 "Structure and function of stator units of the bacterial flagellar motor." 2020.2005.2015.096610.
344 Seemann, T. (2015). "Snippy: fast bacterial variant calling from NGS reads." Internet
345 **https://github.com/tseemann/snippy** (Cited 19 January 2021.).
346 Sudo, Y., H. Terashima, R. Abe-Yoshizumi, S. Kojima and M. Homma (2009). "Comparative study of
347 the ion flux pathway in stator units of proton- and sodium-driven flagellar motors." Biophysics
348 (Nagoya-shi) **5**: 45-52.
349 Takekawa, N., M. Isumi, H. Terashima, S. Zhu, Y. Nishino, M. Sakuma, S. Kojima, M. Homma and K.
350 Imada (2019). "Structure of Vibrio FliL, a New Stomatin-like Protein That Assists the Bacterial
351 Flagellar Motor Function." mBio **10**(2).

Takekawa, N., M. Nishiyama, T. Kaneseki, T. Kanai, H. Atomi, S. Kojima and M. Homma (2015). "Sodium-driven energy conversion for flagellar rotation of the earliest divergent hyperthermophilic bacterium." Sci Rep **5**: 12711.

Terahara, N., T. A. Krulwich and M. Ito (2008). "Mutations alter the sodium versus proton use of a Bacillus clausii flagellar motor and confer dual ion use on Bacillus subtilis motors." Proceedings of the National Academy of Sciences of the United States of America **105**(38): 14359-14364.

Terahara, N., M. Sano and M. Ito (2012). "A Bacillus Flagellar Motor That Can Use Both Na+ and K+ as a Coupling Ion Is Converted by a Single Mutation to Use Only Na+." Plos One **7**(9).

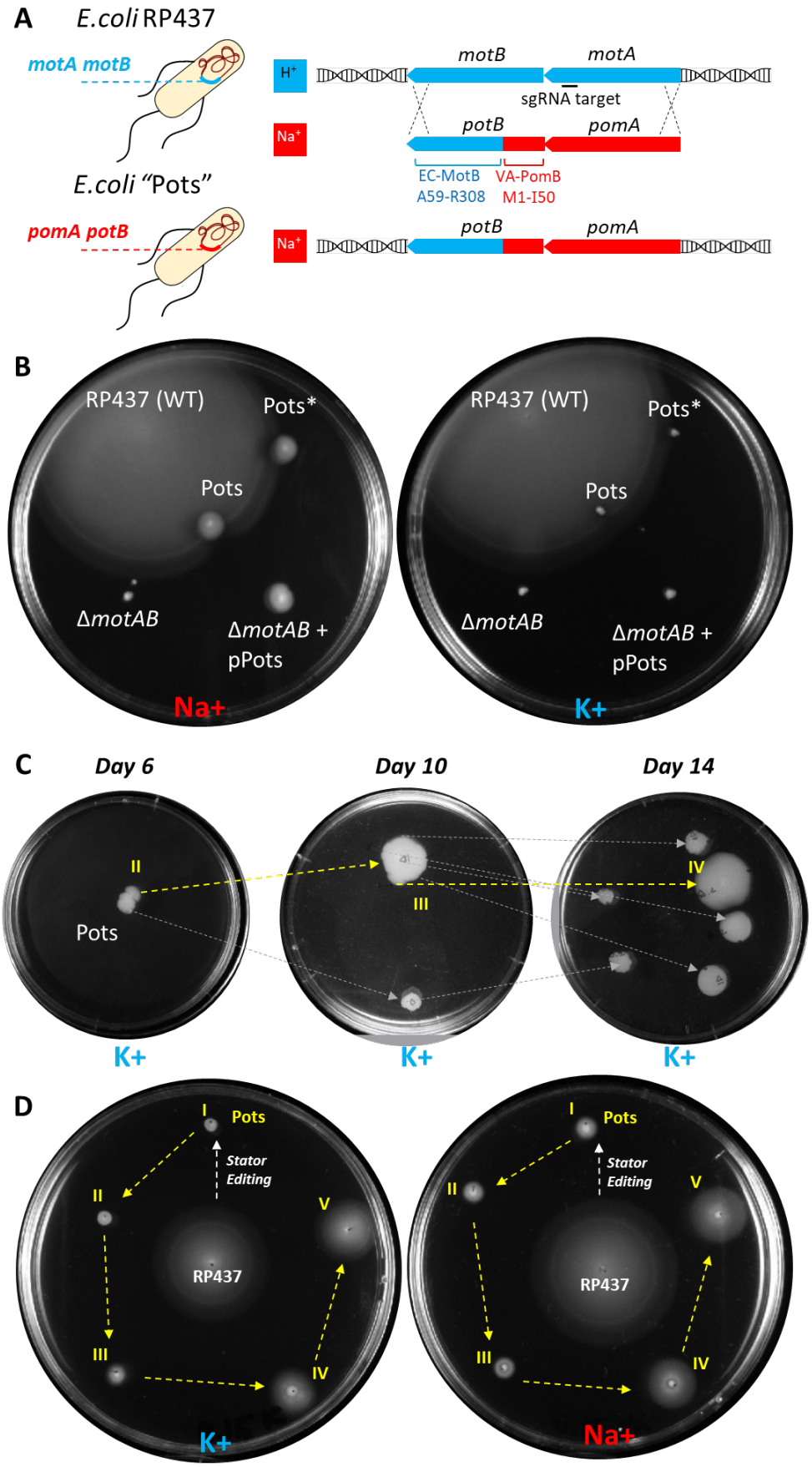

Figure 1. BFM stator editing and recapitulated directed evolution. A) Cartoon of E. coli RP437, carrying a proton-powered stator set (m*otA motB*), undergoing an homologous recombination-catalysed editing process to replace motAB with the

364 sodium-powered chimeric stator *pomA potB* (‘pots’) via a dsDNA donor. The chimeric
365 pots construct consists of PomA from V. alginolyticus (VA) and a spliced B subunit
366 made of Vibrio PomB amino acids M1-I50 fused in frame to E.coli (EC) MotB A59 -
367 R308 (now PotB A51 – R300). B) Soft agar swim plate assay to assess bacterial
368 motility. The strains indicated above were inoculated on 0.3% Agar prepared with
369 either NaCl LB (left) or KCl LB (right) media and incubated at 30°C for 24hrs. The
370 plates contain no antibiotics and 0.4% Arabinose to induce expression from pPots.
371 Strains: RP437 (WT, parent strain), Pots* (not-fully cured, carries plasmid pCas9cr4),
372 Pots (cured of all plasmid), ΔmotAB (E.coli RP6894) with or without pPots (pSHU1234,
373 Cm^+, encoding the PomA PotB construct under control of an inducible Arabinose
374 promoter). C) Directed evolution experiment plates. A single Pots colony was
375 inoculated on a K^+ soft agar plate and incubated at 30˚C until flares developed. The
376 edge of the flare was then transferred onto a fresh plate and allowed to spread radially
377 until at 4-day intervals. Yellow arrows indicate an improved swimmer subpopulation
378 being propagated. Grey arrows indicate other portions of the colony being propagated.
379 D) Full recapitulation of the evolved lineage shown in C. Lineage members were
380 inoculated on soft LB agar with or without sodium from glycerol stocks and incubated
381 24hr at 30°C. Parent strain RP437 is also included in the centre of the plate as control.
382 The phenotypic effect of stator replacement is highlighted by the white arrows.
383 Passages 1 to 5 of the directed evolution experiment are indicated in roman numerals
384 and each passage highlighted by yellow arrows. These passages correspond to: I =
385 Pots, II = L4.2, III = L5.3, IV = L6.4 and V = L6.5 in Fig. 2, respectively.

386

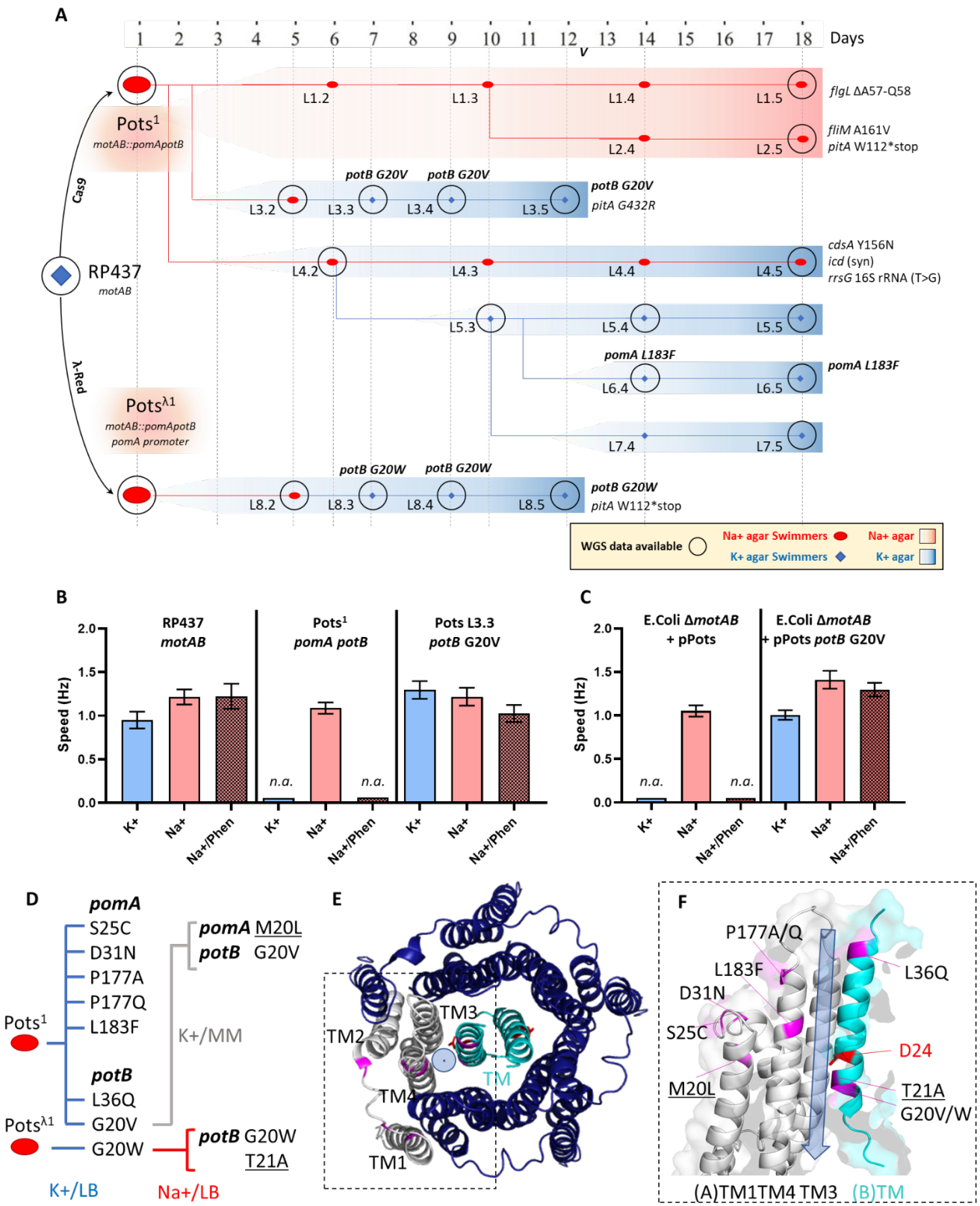

Figure 2. Whole genome sequencing (WGS) of evolved lineages and phenotyping. A) Schematic of directed evolution experiments. The lineage members in the diagram are color-coded based on their ability to swim on either a Na^+ -based substrate (red ellipse) or K^+-based swim agar (blue diamond). All lineage members labelled in blue retained their ability to swim on Na^+-rich soft agar. Lineages passaged

392 on K^+ agar are highlighted by a blue gradient bar, while lineages passaged on Na^+
393 agar are highlighted by a red gradient bar. All strains were locally Sanger sequenced
394 at the *pomApotB* locus, but 21 strains, indicated by black circles, underwent whole
395 genome sequencing (WGS). Lineage number and passage are indicated: ie L1.3
396 indicates the first lineage and the third passage of a motile flare from an initial
397 inoculation site. SNPs identified via variant calling relative to reference genome of
398 MG1655 are annotated next to each respective lineage member. Highlighted genes
399 other than *pomA* and *potB*: *pitA* (metal phosphate:H($^+$) symporter), *flgL* (flagellar hook-
400 filament junction protein 2), *fliM* (flagellar motor switch protein), *cdsA* (cardiolipin-
401 diglyceride synthase), *icd* (isocitrate dehydrogenase), *rrsG* (16S ribosomal RNA). B)
402 Single cell speed measurements using the tethered cell assay measured in Hz
403 (revolutions/s). Blue bar indicates speed in 67 mM KCl motility Buffer, red bar: 85 mM
404 NaCl motility Buffer; red patterned bar: 85 mM NaCL + 100 μM phenamil motility
405 buffer. Number of cells analysed per condition (from left to right): RP437: 27, 51, 25;
406 pots: n.a, 78, n.a; pots *potB* G20V 45, 36, 39 (n.a. indicates no visible rotating cell).
407 Error bars indicate S.E.M. C) Single cell speed measurements using the tethered cell
408 assay in RP6894 Δ*motAB* strain co-expressing *pomA* and *potB* G20V from pPots
409 plasmid. Blue bar indicates speed in 67 mM KCl motility buffer, red bar: 85 mM NaCl
410 motility buffer; red patterned bar: 85 mM NaCl + 100 μM phenamil motility buffer.
411 Number of cells analysed per condition (from left to right): (Δ*motAB* + pPots: n.a., 32,
412 n.a; Δ*motAB* + pPots *potB* G20V: 40, 63, 48). Error bars indicate S.E.M. D) Graphical
413 summary of stator gene mutations detected across all directed evolution experiments
414 and the growth conditions under which these mutations arose. LB indicates agar
415 containing Yeast extract and Tryptone. MM indicates agar in minimal media. Mutations
416 in a subsequent generation are underlined. E) View from the extracellular side of the
417 transmembrane portion of B. subtilis $MotA_5B_2$ stator complex (PDB: 6YSL). One
418 monomer of subunit A is coloured in white and the TM domains of the B subunits are
419 coloured in cyan. Mutant sites obtained in the directed evolution experiments are
420 labelled in magenta, the catalytic aspartate residue essential for function is highlighted
421 in red. The light blue circle indicates the predicted location of the ion transport pore
422 (inward conduction). F) side view of the area highlighted by the dashed box in E.
423 Homologous residue location derived from protein sequence alignments. Primary
424 mutation sites are indicated in black, while secondary mutation sites are underscored.
425 The arrow at the interface between (A)TM3-4 and (B)TM indicates the predicted
426 location of the ion transport pore.